NCSX
Design Basis Analysis

Analysis of NCSX Integrated Structure

NCSX-CALC-14-003-00

November 2, 2006

Prepared by:

_____
H. M. Fan, PPPL

☐

I have reviewed this calculation and, to my professional satisfaction, it is properly performed and correct. I concur with analysis methodology and inputs and with the reasonableness of the results and their interpretation.

☐ **Reviewed by:**

_____
A. Brooks, PPPL

Analysis of the NCSX Integrated Structure

1.0 Executive Summary

This report documents a nonlinear FEA model for NCSX coil support structure and its analytic results for the four loading cases, representing four stages during NCSX operation. The four stages are dead load (DL) only at room temperature, dead loads plus cool-down to 85° K, dead loads plus cool-down and electromagnetic (EM) loads at 85° K, and dead loads and EM loads. The last load case assumes the thermal strain during pulse will cancel the cool-down strain. The analyses do not consist of seismic loads, the interacting loads from other components, and the TF coil preloads.

As the previous nonlinear analysis [1] for the modular coil (MC) and the modular coil winding form (MCWF) indicated the trouble areas at the MCWF joints for the cool-down and EM loads, it is important to make analyses with a model that includes the TF structure and loadings that consider all governing load cases. Due to the physical memory of the existing PC (32 bits with 1.5GB), the modeling efforts required to keep the model size within a acceptable limit. Therefore, the element size for most parts do not have fine mesh pattern. The parts that have few contributions to the stiffness of the integrated system, such as the vacuum vessel and the center stack, were disregarded in the model. However, the load impact from those parts should be considered in the analysis. The model did not contain the modular coil clamp assembly because of its modeling complexity and less input to the modeling stiffness. Alternatively, the modular coils were bonded to the winding forms for stability. The model consists of MCWF system, TF structure system, and all modular coils, TF coils, PF4, PF5 and PF6 in one field period, which is a 120-degree sector.

The FEA model was formed using contact elements among all connecting parts. All the contact surfaces are assumed to be bonded except the MCWF wing interfaces that have frictionless unilateral contact behaviors. The nonlinear property at the wing interfaces offers more rational assessment of the forces across the MCWF toroidal joints. Using less nonlinear elements will utilize less disk memory, reduce running time, and minimize the difficulty for the solution convergence.

The highest MC conductor currents of the current waveforms at full operating capability as shown in Section A.2.3.2 of Reference [2] were selected as the governing case of EM loads. Additional load cases may be run to verify whether the present case is the worst case or not. For the vacuum-pressure impregnation (VPI) modular coils, the relative cooling shrinkage of coil strain has been assumed to be 0.0004 m/m from the room temperature to the operating temperature of 85K.

The NCSX structure will be supported at three locations, 120 degrees apart at the C-C joints [3] to keep the EM loads from the support. Each support offers only the vertical and toroidal restraints and let the structure move freely in the radial direction. The design of base support is not complete yet. For convenience, the base support was located below the outboard stiffening leg.

The exact simulation of the integrated structure, which involves bolt preloads, partial-bolted joints, sliding interfaces, and indefinite orthotropic material properties of the modular coils, was very tedious and may have difficulty of nonlinear convergence. This model shall be treated as a basic model that provides the capability for further modifications of the modeling assumptions. Because of time limit, no further adjustments have been run. In order to obtain conservative answers for particular areas, it is recommended that additional runs should be carried out by modifying some

contact surface behaviors or the material properties. The following results are derived from the current modeling assumptions.

- For 2T high beta scenario, the maximum flux density is 4.901 Tesla on the MC Type B.
- The net centering EM force Fr in one field period from MC is 5 MN.
- Radial preloads for the TF coils is not considering in the analysis. Current design concept indicates that the preloads will be counter balanced by the ring tension of the inboard TF structure.
- The impact of EM loads on the MCWF is much greater than the dead weight and the cooldown thermal strain.
- The maxim displacement is 2.604 mm, occurred at the modular coil Type B from the DL and EM loads. The maximum displacement in the MCWF is 2.371 mm, located near the maximum coil displacement in the shell Type B.
- The maximum von Mises stress in MCWF is 220 MPa (31.9 ksi), found at the inboard location of the shell Type A for dead load plus EM load. The allowable stress of stainless steel casting [15] for the membrane plus bending is 322.5 MPa (46.78 ksi).
- The highest longitudinal stresses of the modular coil is 139MPa (20.1 ksi) in coil Type A from the load case of DL and EM with cool-down effects.
- The PF4, PF5, and PF6 are constrained by the TF structure. Displacements of the integrated structure, especially the vertical displacements, have some impact on their stresses.
- TF and PF currents are not the highest currents. The stresses in this EM load case do not stand for the critical load case for the TF and PF coils and possibly the TF structure.
- No EM loads enter into the base support. All four load cases post the same vertical support reactions, which is 339.4 KN (76.3 kips).
- The contact pressures on the wing bags are not very uniform. With modulus of elasticity at 13,750 MPa, the maximum contact pressure is 128 MPa (18.6 ksi.), occurred on the wing bag Type B. The pressure could be improved if shape is changed to provide more uniform compression.
- The TF structure will help carrying some loads to the base support, if the TF structure sections are fully bonded at the shim joints.
- The thermal strain from the cool-down has only small impact on loads at flange joints in comparison with the EM loads.
- Based on the net bolt preload of 45797 lbs for the 1 3/8" bolt, several locations along the toroidal flange joints have shear forces far exceeds the allowable value. That might cause the joints to slip.
- In evaluating the bolt joint capacity, the selected areas for the bolt group shall be small enough that the centers of bolt groups match closely with the centers of bolt loads.
- The worst location for the joint slip in the MCWF is at the inboard flanges joint B-C.
- A complete design of the bolt joint should also consider the impact of preload change due to thermal variation and the creep of the insulation materials.
- The model assumed all contact surfaces were bonded except for the wing interfaces that used frictionless contact elements through the wing bag shims. In the real case, the modular coils, TF coils, and PF coils are not exactly bonded to the structure. Some bolt joints may not be firmly connected. It is recommended that additional runs by changing contact behaviors or modifying the material properties shall be performed to assess the impact of modeling assumptions.

2.0 Assumptions

The following assumptions were applied in the analysis:

The model was built on the Pro/E model. All the part contact surfaces are assumed to be bonded except the MCWF wing interfaces. The wing bag shim was bonded to shell on one side and had frictionless contact behaviour to the adjacent shell on the other side. With primary interest in the forces on the MCWF joints, the frictionless contact elements properly imitate the forces that transfer through flange joints at wings.

All material properties of coil conductors are based on the smeared properties. As the MC conductor test programs have not yet established many of the required data to form an orthotropic property, the model utilized isotropic material properties for the winding packs. As the coils are continuous in the axial direction, the isotropic material properties are more suitable to be represented by the test data in the longitudinal direction. The isotropic properties are also used for the TF and PF coils.

The model did not contain the modular coil clamp assembly because of its modeling complexity and less stiffness contribution. To ensure the stability of the modular coils in the model, they were bonded to the winding forms. Two longitudinal shear moduli in the coils were reduced to limit the shear impact on the contact surfaces and lower the composite action with the MCWF. The shear rigidities of shims for the TF and PF coils are decreased for the intention of less resistance to the coil movements. A description of the FEA model was given in a PowerPoint document [4].

To minimize the size of the model, the model disregarded the parts that have few contributions to the stiffness of the integrated system, such as vacuum vessel and center stack. However, their load impacts were added in the solution phase. For conservative reason, the weight of center stack was supported at the upper TF structure and the weight of vacuum vessel assemble was hung from the upper side of the shell Type A.

To make sure an adequate wedge action for the TF coil, all TF coils will be preloaded by pulling in the radial direction against the TF structure. As this assembling procedure will be carried out before the TF structure is tied down to the MCWF, these preloads will not transfer to MCWF and will not be considered in the analysis.

No bolt holes and bolt connections were simulated in the model and no bolt preloads were applied in the analysis. The normal forces and shear forces across the bolt joints shall be calculated after the analysis for establishing the required bolt preloads that will make sure that the bolt joints will not be opened up or sliding.

At the discussion meeting [3] of the stellarator support structure, the notes showed that the structure will be supported at three locations, 120 degrees apart at the C-C joints. The supports offer cyclically symmetric restraints of weight and seismic loads, but no EM loads. For this purpose, only the vertical and toroidal restraints exist on each support.

As the design of base support structure is not completed yet, fictitious base support blocks were added beneath the integrated model to keep high local stress and deformation away from the structure.

3.0 Analysis Methodology and Inputs

3.1 Methodology

The analysis uses the same mesh pattern for EM and stress analyses so that it is able to avoid the errors of mapping applied loads from one model to another model. The procedure will first solve the electromagnetic (EM) analysis and review the results. Then applying the EM loads obtained from the first analysis to the structural analysis for evaluating the stresses and displacements.

Because of cyclic symmetry in the geometry and the loading, the model is formed in a 120-degree sector to minimize the model size and the computer running time. Figure 3.1.1 and 3.1.2 show the models elected for the EM analysis and the structural analysis, respectively. The geometric nonlinearity of the contact behavior, caused by the wing interfaces, was solved using the ANSYS nonlinear method.
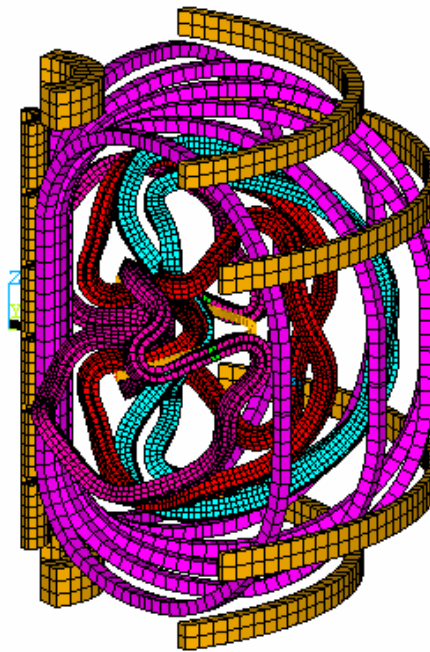
Fig. 3.1.1: EM model consists of MC, simplified plasma, PF coils, and TF coils

5
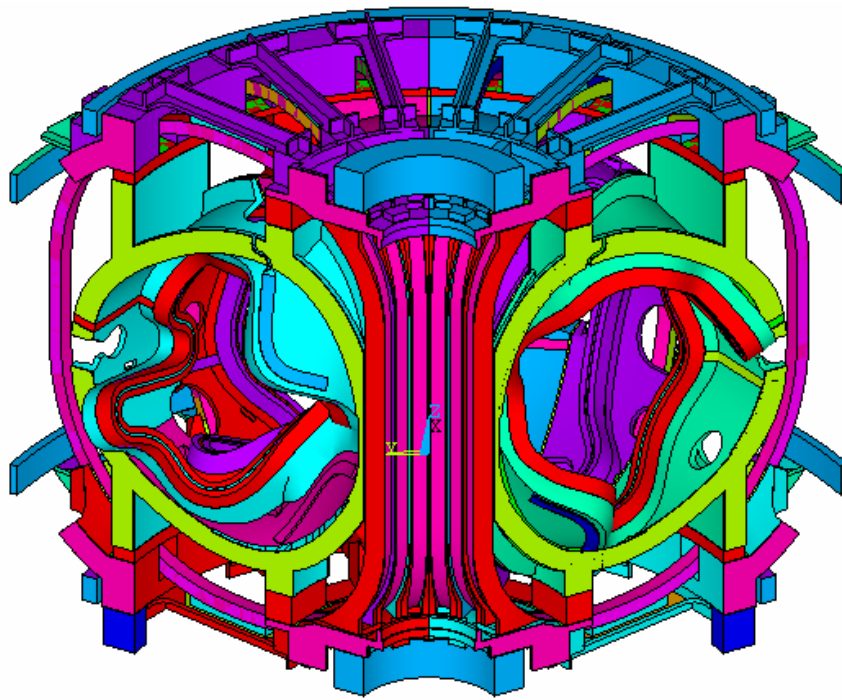
Fig. 3.1.2: Integrated structural model

3.2 Inputs of Models

The geometric files of the MCWF and modular coils were developed by ORNL while the geometric files of the TF structure and TF and PF coils were provided by PPPL. Some small features, such as bolts, bolt holes, chamfers, and fillers in the geometry were removed prior to the meshing.

In the EM model, the PF coils, TF coils, and the modular coils are formed by ANSYS 8-node solid element SOLID5. For the current input, the modular coils and TF coils were cut near the mid-height at the outboard legs. The plasma current was simplified by SOURE36 current elements along the center line of the plasma current.

After the EM analysis, the SOLID5 elements for the winding packs were shifted to structural 3-D SOLID45 elements with identical number for the nodal points and elements. The final structural model consists of the following components:

1) Modular coils
2) MC winding form (MCWF)
3) MCWF poloidal breaks
4) MCWF toroidal shims
5) MCWF wing bag shims
6) PF coils No.4 to No.6
7) PF coil brackets and shims
8) TF coils
9) TF coil shims at inboard, outboard, top and bottom
10) TF inboard wedge spacers
11) Inboard TF structure
12) Outboard TF structure

6

13) Tie bars for (11) and (12)
14) TF structure toroidal shims
15) Connecting blocks between TF structure and MCWF
16) Fictitious base support blocks

 The number of nodes and elements of the model was examined in order to form a final model that can fit into the 3.2 bit PC with 1.5GB total physical memory. All contact regions used the surface-to-surface contact elements. Even with a total number of 163,090 elements and 283,750 nodes, the model does not have fine mesh size.

The model needs appropriate boundary conditions and support constraints to simulate the structure in a stable and cyclically symmetric condition. For parts with identical boundary nodes on θ=+60° and the θ=-60°, such like MCWF and PF coils, coupled degrees of freedom were defined for all degrees of freedom. For those without identical boundary nodes in the TF wedges and TF structure, the constraint equations were generated. Figure3.2.1 shows the model with boundary condition, in which the green color and the pink color indicated the coupling and constraint equation, respectively. To be able to achieve the cyclically boundary condition, all nodes on the boundary surfaces shall be rotated into the same global cylindrical coordinate system. The cyclically symmetric conditions were also required for the wind bags located outside the end boundaries on the shell Type C. The detail arrangement has been explained in the previous report [1].

Fictitious base support blocks were added beneath the integrated model to keep high local stress and deformation away from the structure. The model was restrained by one-nodal support that has vertical and toroidal constraints on the fictitious block. All the measuring units in the model are in international MKS system.
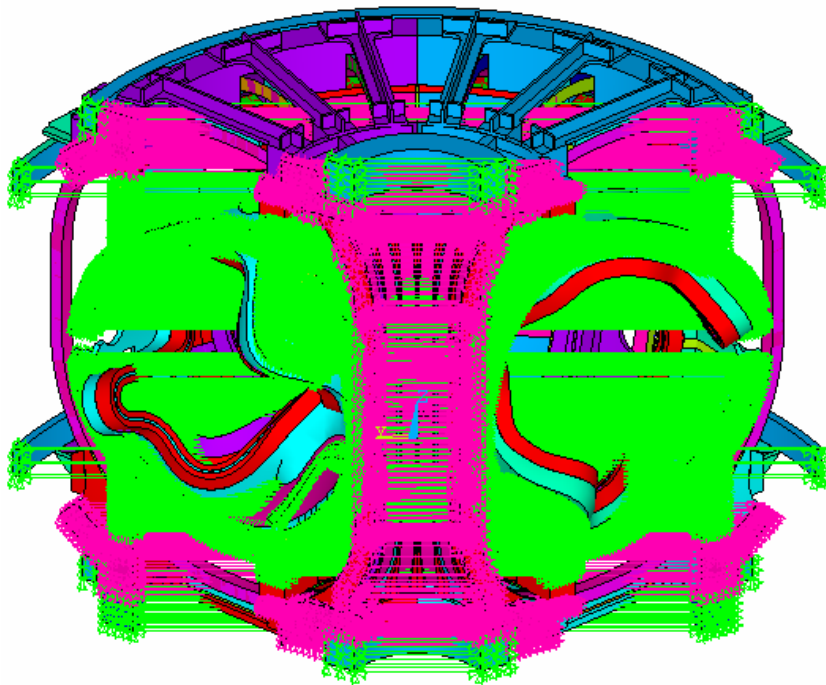
Fig. 3.2.1: Cyclic Symmetry Between θ=-60° and θ=+60°

3.3 Applied Coil Currents for EM Analysis

Reference [2] presents coil operating capability including turn per coil and all current waveforms. The listed current is the current in each turn, not the current in each conductor. Therefore, the modular coil currents will be the currents multiplied by the number of conductor turns. Table 3.3.1 lists the number of coil turns and turn currents at the full operation capability for the 2T high beta scenario that was selected in the EM analysis.

Table 3.3.1: Turn number of each coil set

Coil	M1	M2	M3	PF1	PF2	PF3	PF4	PF5	PF6	TF	Plasma
Turn No.	22	22	20	72	72	72	80	24	14	12	1
Turn Current	37190	37783	36538	-14615	-14615	-9054	-7498	460	453	-1301	0

For the current convention system, NCSX utilizes the cylindrical coordinate system with the Z-axis as vertical. A positive PF or plasma current is in the direction, which is counter-clockwise viewed from above. A positive poloidal current, such as TF or modular coil current, flows in the positive Z-direction in the inner leg.

3.4 Applied Loads for Structural Analysis

The individual loads are EM loads, cooling strain, and deal loads that including interface dead load from vacuum vessel and center stack. The cooling strain is the relative strain between modular coils and MCWF due to temperature changes during the modular coil VPI process and the initial cooling to the operating temperature of 85K. R & D test has indicated that the winding pack cure shrinkage is very small and negligible. The other test result shows that the CTE of the winging pack is slightly higher than the winding form and when the modular coil is cooled to 85K, the relative thermal strain between the modular coil and the winding form is about -0.04%.

To simulate the load case of cool-down of the modular coils, the equivalent temperature drop of 23.26K that is equivalent to coil strain of 0.04%, should be applied to the WP only. The temperatures on the other parts were kept unchanged.

To apply gravity load, specify gravity acceleration in a positive Z direction by using ACEL command. As the model does not contain vacuum vessel and center stack, the appropriate weight shall be added at the part interfaces. One third of center stack weight [5] is 1288.4 lbs (5731 N) and one third of vacuum vessel weight [6] is 4912.5 lbs. The weight of inside vessel components was estimated about 2000 lbs.

The structural analysis shall consider all possible loading combinations to determine the governing load case. Four load cases were defined in the analysis. They are (1) dead load only at room temperature, (2) dead loads plus cool-down to 85° K, (3) dead loads plus cool-down and EM loads at 85° K, and (4) dead loads and EM loads. The last load case assumes that the thermal strain during pulse will cancel cool-down strain.

Radial preloads for the TF coils was not considering in the analysis. Current design concept indicates that the preloads will be counter balanced by the ring tension of the inboard TF structure.

To accomplish this condition, the TF coils shall be preloaded before the TF structure attached to the MCWF.

3.5 Material Properties

The material properties are represented by isotropic materials with some modifications on the shear modulus of elasticity to consider the parts that are formed by the composite materials or possible surface sliding. The modular coil R & D test results [7] illustrate the flexural modulus of elasticity of the winding pact at 77K varies from 11.08Msi (76.4GPa) for bare Cu specimens to 7.37Msi (50.8GPa) for glass wrapped specimens. The longitudinal compressive test at room temperature [8] shows the modulus of elasticity at an average value of 9.11Msi (62.8GPa). As the test program has not yet established all of the required data for forming an orthotropic property, the analysis employed the smeared isotropic material property with a reduced longitudinal shear modulus of elasticity to consider the impact of possible contact sliding from the winding form.

The elastic modulus of MCWF casting alloy shall meet 145GPa at 77° K [9]. The flange shim insulations placed between toroidal flange joints are formed with a 3/8-in SS covered by 2 layers of 1/16-in G11. The equivalent isotropic properties were calculated for their material properties. The casting TF structure has not completed the design yet. Its elastic modulus was assumed to be the same as the MCWF. Table 3.5.1 summarizes the material properties of all components. In the Table, the shear modulus G with a sign of "*" is calculated from the isotropic material relationship. The shear rigidities of shims for the TF and PF coils are decreased for the intention of less resistance to the coil expansion movements. For the modular coils, the longitudinal direction is Z for the element coordinate system. The 1st shear modulus is for Gxy and the 2nd shear modulus is for Gyz and Gxz. The much small values for the Gyz and Gxz intend to limit the shear impact on the contact surfaces and lower the composite action with the MCWF.

Table 3.5.1: Material properties of components

	E (MPa)	G (MPa)	CTE (m/m/°K)	Density (kg/m^3)	Poisson's Ratio
MCWF	145,000	*	1.700E-05	7750	0.31
Modular coil	63,000	26250 / 525	1.720E-05	8500	0.20
MCWF toroidal shim	150,000	*	1.700E-05	7750	0.27
MCWF poloidal shim	193,000	*	1.700E-05	7750	0.31
MCWF wing bag	13,750	*	3.000E-05	1820	0.32
Wing bag image	6,894	*	3.000E-05	0.1	0.32
PF coil	120,000	*	1.600E-05	8300	0.33
PF6 coil bracket	193,000	*	1.700E-05	7750	0.31
PF coil support shim	22,000	440	1.720E-05	1900	0.21
TF coil	120,000	*	1.600E-05	8300	0.33
TF coil side shim	22,000	440	1.720E-05	1900	0.21
TF coil top/bot shim	95,000	950	1.700E-05	7750	0.31
TF coil wedge spacer	145,000	*	1.700E-05	7750	0.31
TF structure	145,000	*	1.700E-05	7750	0.31
TF structure tie bar	145,000	*	1.700E-05	7750	0.31
TF structure shim	22,000	*	1.720E-05	1900	0.21
Connecting block	145,000	*	1.700E-05	7750	0.31
Base support block	193,000	*	1.700E-05	7750	0.31

4.0 Results and Interpretations

4.1 EM Analysis

Figure 4.1-1 demonstrates the flux density contour plot, in which the maximum flux density is 4.901 Tesla in the modular coil. The maximum flux density equals to the value of the previous analysis [1] which has same currents in the modular coils and the TF coils. The currents in the PF coils have some variations.
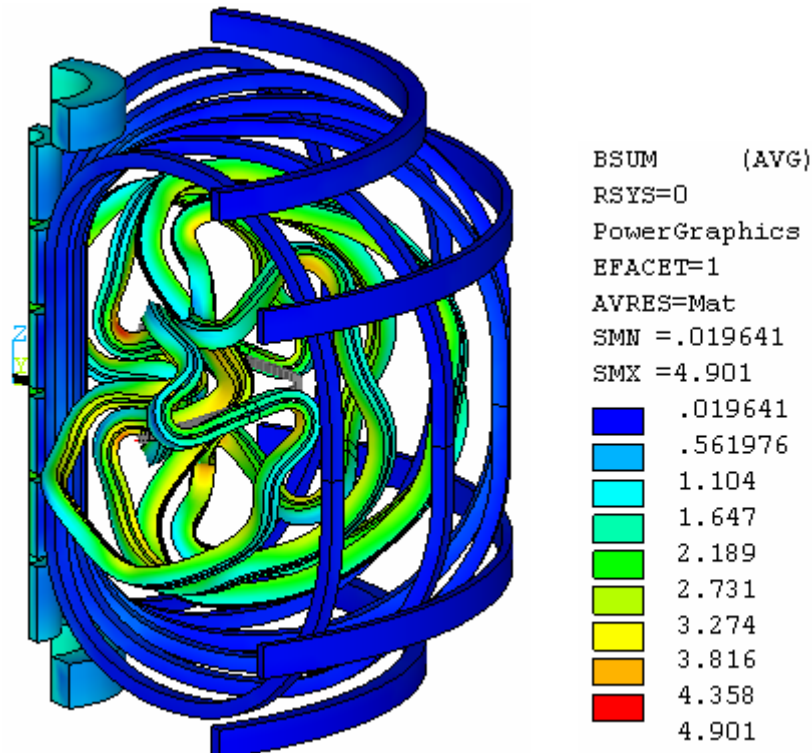
Fig. 4.1-1: Flux density contour plot

Figure 4.1-2 displays the magnetic forces that show the magnetic forces in the TF, PF5, and PF6 coils are very small in comparison with the forces in the modular coils. Because of the stellarator stmmetry, the net EM force components in the vertical and toroidal directions are equal and opposite for the three right-hand-side modular coils and the three left-hand-side modular coils that result in net zero forces.
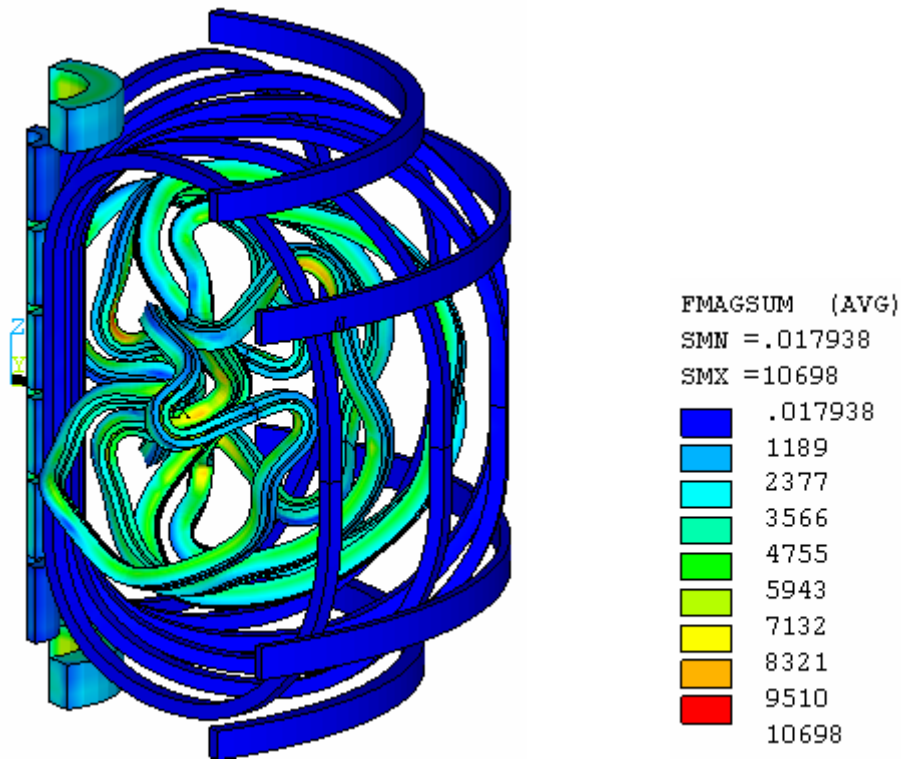
Fig. 4.1-2: Element vector forces of Type B modular coils

4.2 Structural Analyses

Four load combination cases representing four stages during operation as shown in Section 3.4 were run in the analyses. As the interest in the analysis will be focus on the MCWF joints, the results will put emphasis on the MCWF structure and the toroidal flange joints.

4.2.1 Displacements

The cool-down displacement calculation was based on the relatively thermal strain between the modular coil and the winding form, from which the thermal stresses were induced. The free thermal displacement from the room temperature to the 85K that does not generate thermal stresses in the structure did not include in the analysis and the following displacement values.

The integrated structure is supported at the edge of the outboard leg with vertical and toroidal constraints. The maximum displacements of the four load cases are illustrated in Table 4.2.1.1. For the dead load, the maximum displacement occurs at the mid-section between supports. During the cool-down, modular coils shrink more than the MCWF that causes bending moments in the combined section of MC and MCWF and yields greatest displacement on the wings of MCWF. With the DL and EM loads, the maxim displacement is 2.604 mm, occurred at the modular coil Type B. The maximum displacement in the MCWF is 2.371 mm, located near the maximum coil displacement in the shell Type B.

11

Table 4.2.1.1: Structural Displacements of Four Load Cases

	Dmax (mm)	Uz-max (mm)	Uz-min (mm)
Dead load	0.384	0	-0.384
DL + Cooldown	0.595	0	-0.517
DL + Cooldown + EM	2.559	1.104	-1.318
DL + EM	2.604	1.091	-1.285

The vertical displacement contour plots for the dead load only and the dead loads plus EM loads are illustrated in Fig. 4.2.1.1 and Fig. 4.2.1.2, respectively. The unit of displacement is meter. In the case of only the dead loads (Fig. 4.2.1.1), the vertical displacements are greater in the inboard region than the outboard region. If more evenly distributed displacement is preferred, the location of the supports shall be moved toward the inboard leg. In Fig. 4.2.1.2, the vertical displacements in the right-hand side are opposite to the left-hand side mainly due to stellarator symmetry of the EM loads.
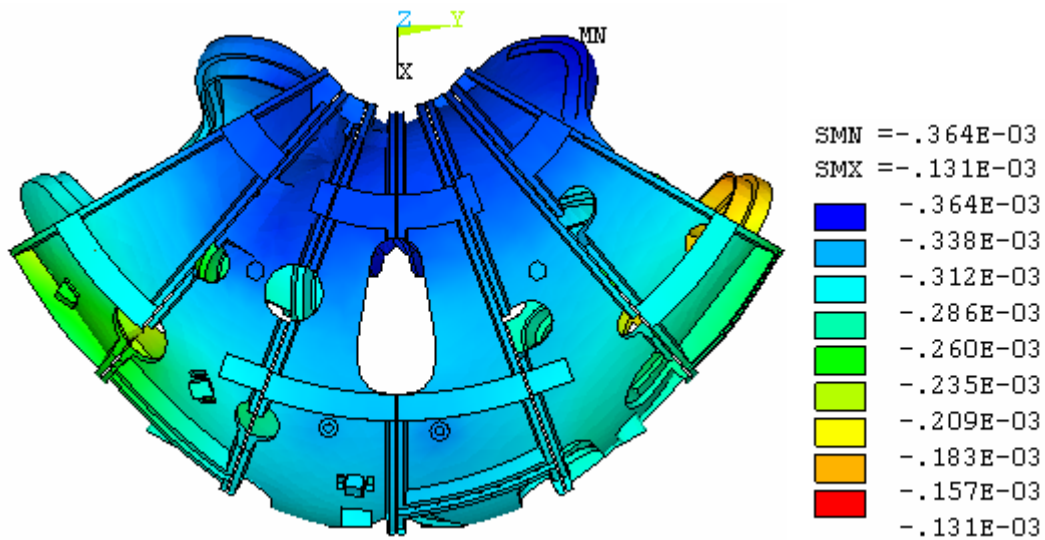
Fig. 4.2.1.1: Vertical displacement (Uz) for dead loads

SMN =-.001136
SMX =.944E-03

-.001136
-.905E-03
-.674E-03
-.443E-03
-.212E-03
.196E-04
.251E-03
.482E-03
.713E-03
.944E-03
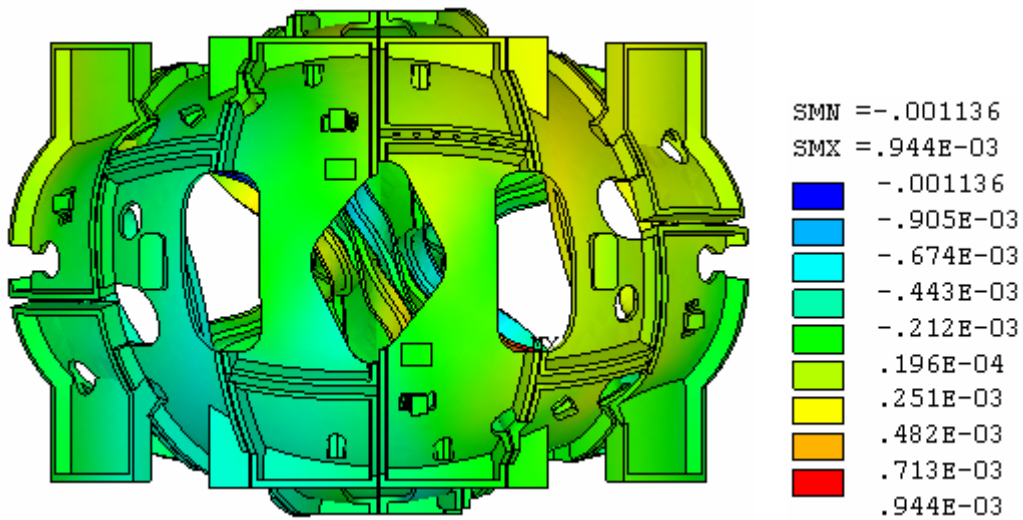
Fig. 4.2.1.2: Vertical displacement (Uz) for DL plus EM loads

4.2.2 Stress in MCWF

A review of the stress results demonstrates the Load Cases 3 and 4 are the leading cases for the structural responses primarily due to the EM loads. Examining stresses on all parts show that the maximum stress takes place at the MCWF toroidal shim AA for the Load Case 4, as shown in Fig. 4.2.2.1. The peak stress is confined locally at the corner of an element and therefore it is not a great concern.

SEQV   (AVG)
DMX =.556E-03
SMN =387553
SMX =.509E+09

387553
.570E+08
.114E+09
.170E+09
.227E+09
.283E+09
.340E+09
.396E+09
.453E+09
.509E+09
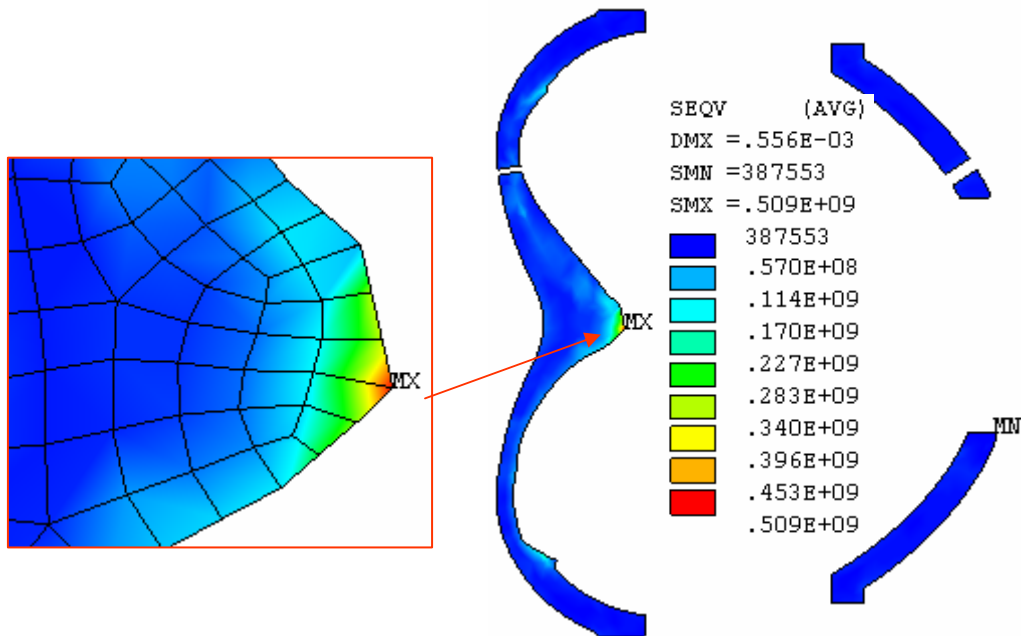
Fig. 4.2.2.1: Peak local stress from DL plus EM loads

For the dead load plus EM load, the von Mises contour stress of the MCWF, which is the major load-carrying element, is shown in Fig.4.2.2.2. The maximum stress of 220 MPa (31.9 ksi) was found at the inboard location of the shell Type A, as shown in the Fig. 4.2.2.3. The peak stress is

13

limited to a small area, near the maximum stress spot on the toroidal shim AA displayed in Fig. 4.2.2.1. The stresses in the other areas are much smaller than the maximum value.
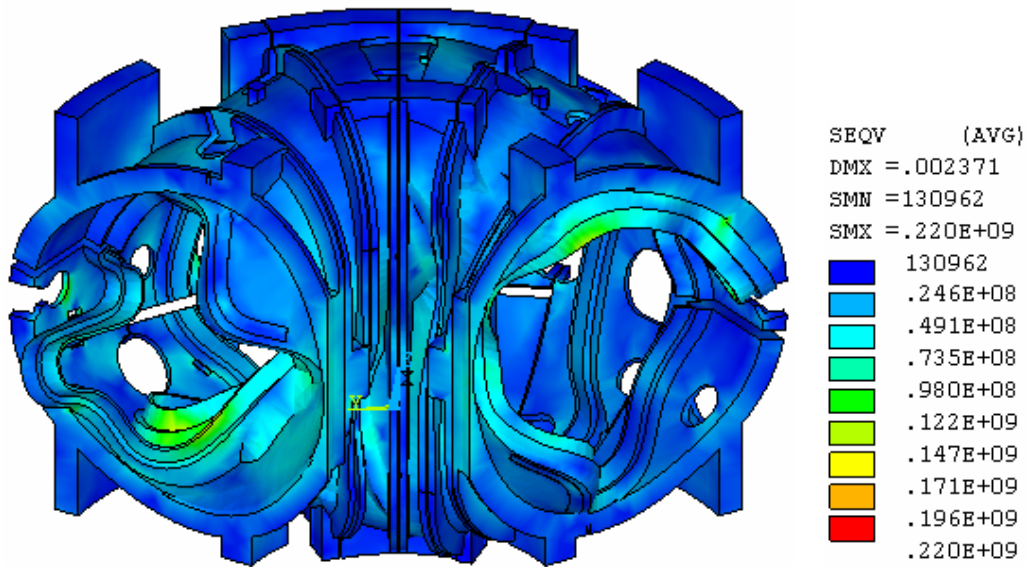
Fig. 4.2.2.2: MCWF von Mises stress from DL plus EM loads
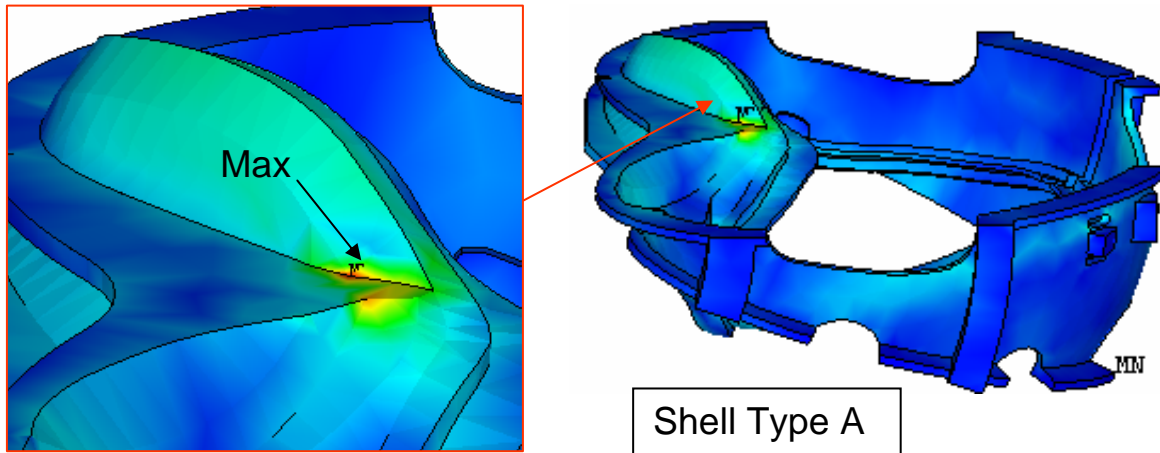
Fig. 4.2.2.3: Maximum von Mises stress from DL plus EM loads

The shell structure is made of stainless steel casting. According to the NCSX design criteria (see Ref. [12]), the allowable stress for the membrane plus bending will be 322.5 MPa or 46.78 ksi [15], which is larger than the maximum stress.

4.2.3 Stress in Coils and TF Structure

On the base of the selected material properties and the assumed bonding contact behavior, the longitudinal stresses contour plot for the modular coil Type A, which have the highest stress, is illustrated in Fig. 4.2.3.1 from DL and EM with and without cool-down effects. The load case with

14

cooldown yields more tension in the coils than the load case without cool-down because of additional shrinkage in the modular coils than the winding form.

SZ   (AVG)
RSYS=SOLU
DMX =.001855
SMN =-.193E+08
SMX =.816E+08
DL & EM
-.193E+08
-.813E+07
.309E+07
.143E+08
.255E+08
.367E+08
.480E+08
.592E+08
.704E+08
.816E+08

SZ   (AVG)
RSYS=SOLU
DMX =.002559
SMN =-636613
SMX =.139E+09
DL, EM & Cooldown
-636613
.149E+08
.304E+08
.459E+08
.614E+08
.769E+08
.924E+08
.108E+09
.123E+09
.139E+09
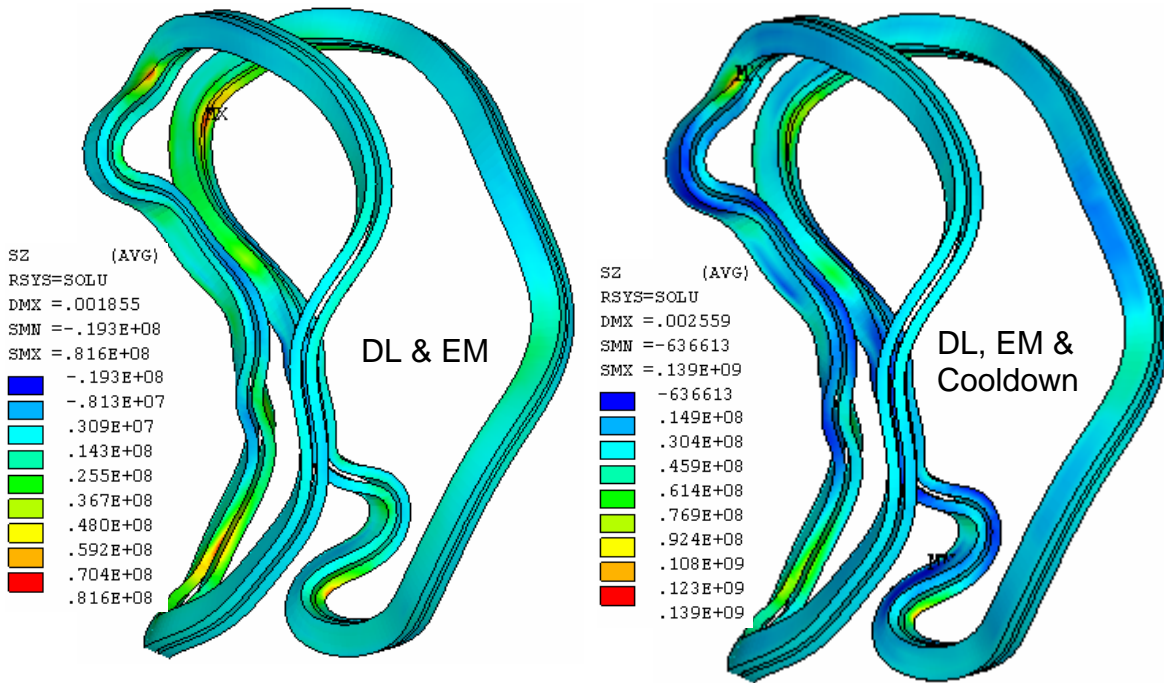
Fig. 4.2.3.1: Axial stress of coil Type A from DL and EM with and without Cool-down

The currents used in the analysis for the PF coils and TF coils do not represent the highest currents in the coils and, therefore, the stresses in those coils are not considered to be the critical stresses. It is noted that the PF coils are constrained on the TF structure. The displacements of the integrated structure, especially the vertical displacements, have more impact on the stresses in the PF5 and PF6. Figure 4.2.3.2 exhibits the axial stress contour for the PF5 and PF6.

SY   (AVG)
RSYS=1
DMX =.717E-03
SMN =-.531E+07
SMX =.745E+07
-.531E+07
-.390E+07
-.248E+07
-.106E+07
357654
.178E+07
.319E+07
.461E+07
.603E+07
.745E+07
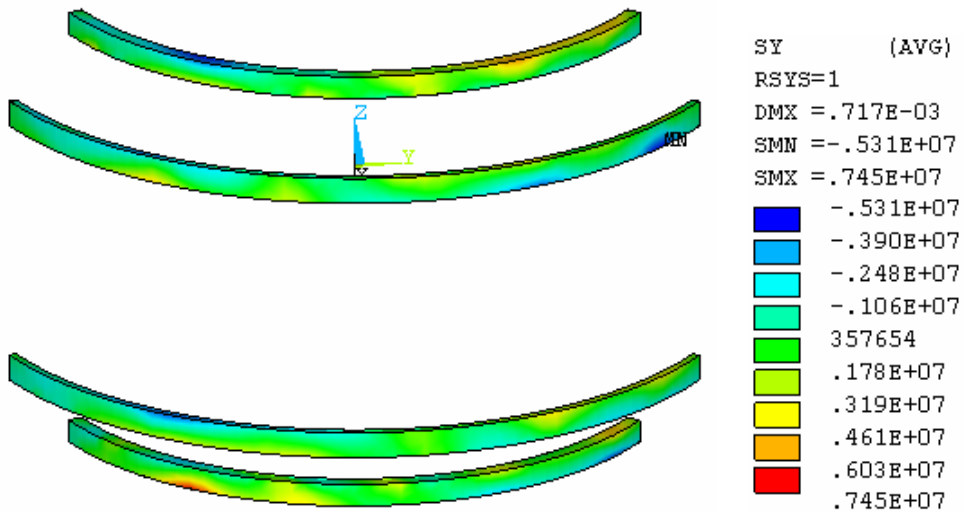
Fig. 4.2.3.2   Axial stress of PF5 and PF6 from DL plus EM loads

The design of TF structure has not completed yet. From the applied DL and EM load, stress contours of the lower TF structure are given in Fig.4.2.3.3. The toroidal stresses are shown on the left side and the von Mises stresses are shown on the right side. The results are not necessary represent the critical load condition due to the input currents. However, it indicated two structural behaviors: (1) the outer TF structure subjected to bending in the toroidal direction under the vertical deformation of the integrated structure, and (2) the maximum stress will be at the lower TF structure near the base support.
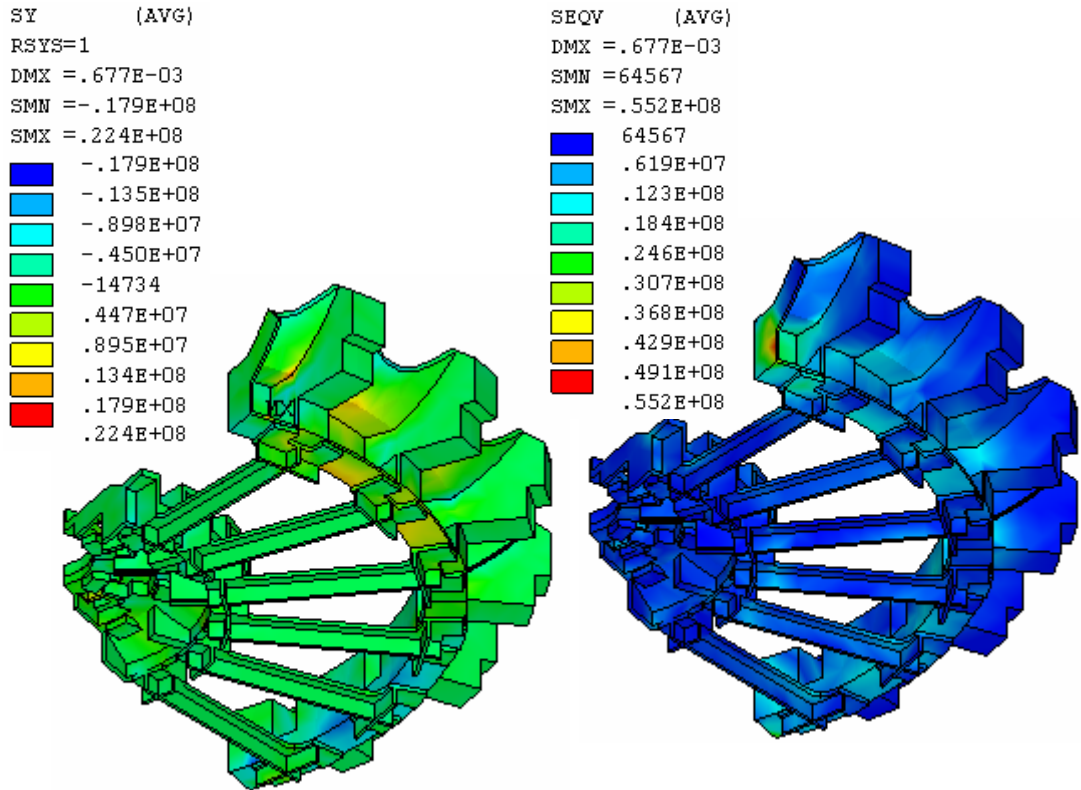
Fig. 4.2.3.3: Axial stress of PF5 and PF6 from DL plus EM loads

4.2.4 Base Support Reactions

The support reactions from the four combined load cases are listed in Table 4.2.4.1. They are only vertical and toroidal restraints at the support. Because of the stellarator symmetry, the EM loads do not transfer to the support. Neither the thermal strain from the cool-down produces loading on the support. The only loading that transfers to the support is the dead load, resulting a vertical reaction of 339.4 KN (76.3 kips).

All four load cases post almost the same reactions. The small force variations in the toroidal direction are caused by nonlinear convergence and FEA model. The nodal points and elements in

the model are not totally symmetric with respect to the middle of the cross section, although the CAD geometries are symmetry.

Table 4.2.4.1: Support Reactions for Four Load Cases

	Fr (KN)	Fθ (KN)	Fz (KN)
Dead load	0	0.074	339.4
DL + Cooldown	0	0.077	339.4
DL + Cooldown + EM	0	0.280	339.4
DL + EM	0	0.283	339.4

4.2.5 MCWF Toroidal flange Joints

The model did not include any bolts or any bolt preloads in the toroidal flange joints. An investigation of MCWF bolt joints [10] was performed by A. Brooks based on the net bolt preload of 45797 lbs for the 1 3/8" bolt. The flange was divided by several regions as shown in Figure 4.2.5.1 in according with the discontinuation in the flanges and at inboard regions without bolt connection (green color). In each region, the normal force and the shear force were evaluated from the FEA results. The required coefficients of friction to prevent slip were then calculated and plotted for all the flange regions.
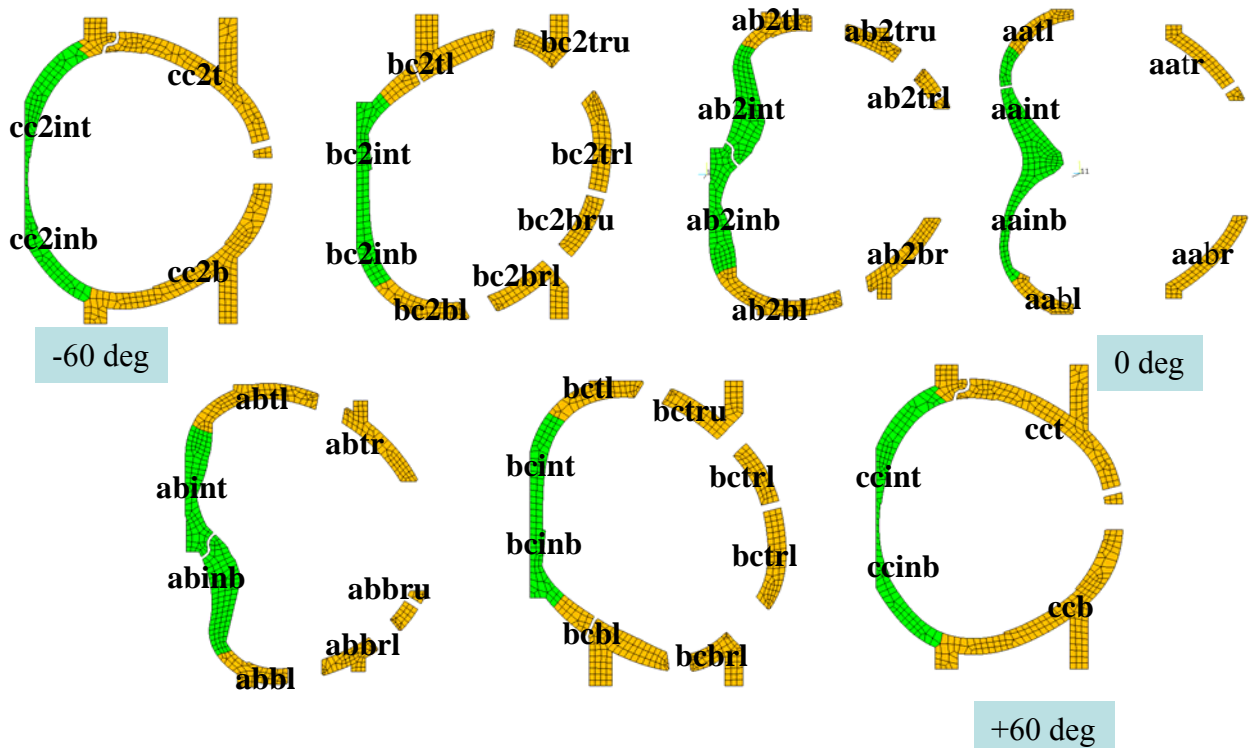
Fig. 4.2.5.1   Designated names in flange regions for selected bolt groups

17

Figure 4.2.5.2 illustrates the coefficients of friction needed [11] to prevent slips for EM load at the MCWF toroidal flange joints from two FEA models, one with MCWF only (red color) and the other with integrated model (blue color). The side-by-side result comparison shows the influence of adding TF structure in the model. Some improvements are found in most of regions. However, the shear forces in many regions are much higher than the allowable coefficient of friction, 0.15, prescribed by the design criteria [12]. The results indicate that the TF structure can assist in carrying loads to the base support, if the TF structure shim joints are fully bonded and good enough to maintain the bending, torsional and shearing stiffness along the longitudinal direction as assumed in the integrated model.
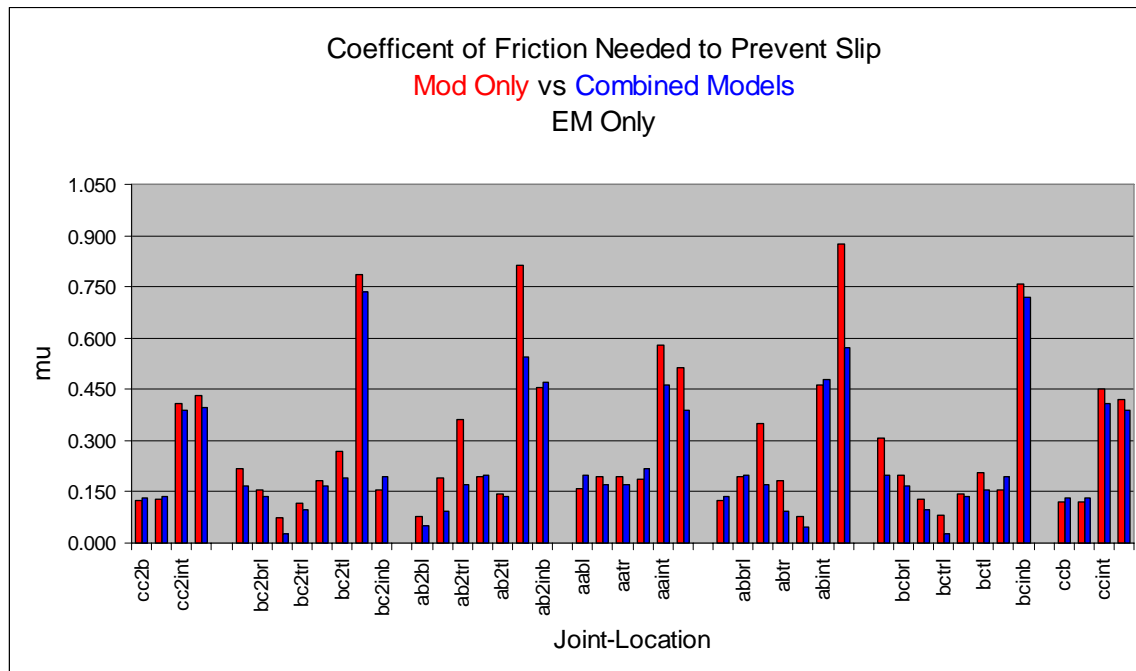
Fig. 4.2.5.2   Comparison of required coefficient of friction at bolt joints for two models with EM only load case

Figure 4.2.5.3 [11] illustrates the coefficient of friction needed to prevent slips on the integrated model that subjected to the dead loads and EM loads with or without cool-down strain. A comparison of the required coefficients of friction shows that the thermal strain from the cool-down has only small effects at flange joints. The worst location for the joint slip is at the inboard flange joint B-C.
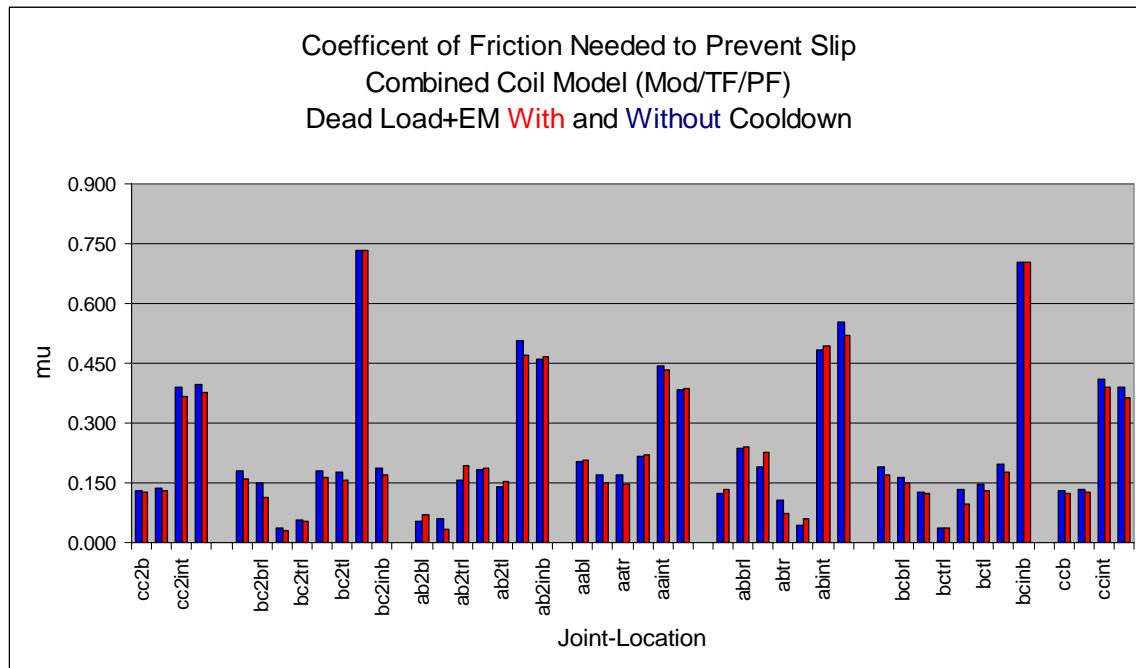
Fig. 4.2.5.3   Comparison of required coefficient of friction for DL and EM load with and without cooldowm.

The approach for calculating required coefficients of friction yields accurate results only when the center of load matches the center of the bolt group in each region. As the joint loads are not uniform along the flanges, the resulting load centers and the bolt group centers, in general, will not be coincident. To avoid obvious discrepancy, it is suggested that some regions should be subdivided into smaller areas, such as regions CCB, CC2B, CCT, and CC2T.

4.2.6 Wing Bags

Wing bag was designed to carry the loads from the wing to the next shell segment. The amount of load transfer depends on the stiffness of the wing bag, the contact behavior and the stiffness of wing. The model assumed wing bag shim was bonded to shell on one side and had frictionless contact behaviour to the adjacent shell on the other side. This is the only nonlinear action in the model in order to predict more appropriate load-transferring mechanism. The analysis presumed that the modulus of elasticity of wing bag was 13,750 MPa.

Figure 4.2.6.1 shows a contour plot of the wing bag contact pressure at the shell Type A for the DL and EM loads. The unit of contact pressure is Pascal. Positive pressure indicates load toward the surface and therefore is in compression. The distribution of the contact pressure is not very uniform on the contact surface. Most effective spot on the wing bag locates near the cantilever end of the wing. The maximum contact pressure is 128 MPa (18.6 ksi.), occurred on the wing bag at shell Types B.
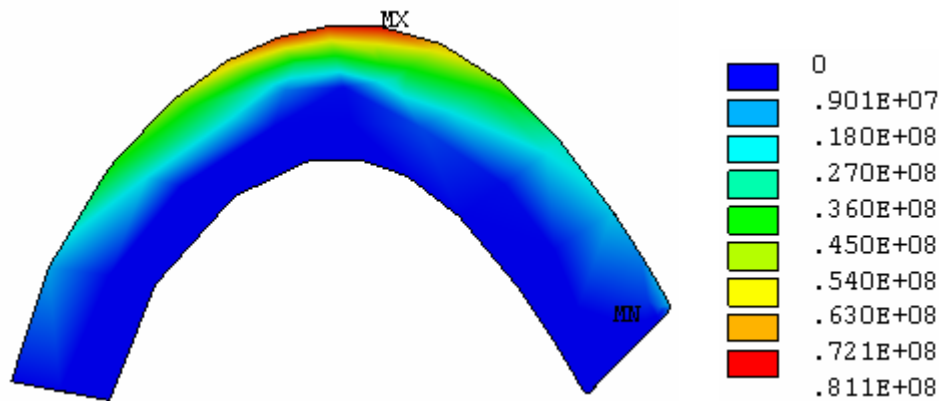
Figure 4.2.6.1:   Contact pressure on wing bag at shell Types A

4.2.7 Commands in Solution Phase

The integrated FEA model database file "file6.db" includes the support constraints and the EM loads for 2T high beta scenario at 0 seconds. When the support location or the EM load changes, the corresponding nodal constraints or the nodal forces should be removed and replaced.

The inputs of dead loads make use of the ANSYS acceleration command "acel' and add in the proper weights from PF coil center stack [13] and vacuum vessel [14].   For conservative, these additional weights are supported on the upper structure. The input commands are:

```
acel,,,9.806
csw=-3865*4.448/6          ! center stack weight/6
f,278757,fz,csw
f,299941,fz,csw
esel,s,mat,,90                 ! vacuum vessel
nsle
nsel,r,loc,z,nz(261533),nz(261533)
f,all,fz,-6900*4.448/32
allsel
```

The relative thermal strain between the modular coils and the winding form is about 0.04% when they are cooled to 85K. By setting up the reference temperature at 0° K, the equivalent modular coil temperature becomes -23.2558° K. The input commands are:

```
tref,0
esel,s,mat,,1,3       ! MC
nsle
bf,all,temp,-23.2558
allsel
```

The displacement criterion was used for the nonlinear convergence criteria. As the load case including EM load was more difficult to converge due to coarse elements, a separate convergence tolerance value was selected depending on the load case with or without EM loads

```
    cnvtol,u,,0.05              ! without EM loads
or
    cnvtol,u,,0.05*2.1          ! with EM loads
```

5.0 Discussions

A FEA model of integrated structure was created with the main interest in studying the MCWF joints during the operation stages. As previous model did not include the TF structure, it is essential to understand what will be the impact on the MCWF joints by adding the TF structure.

In order to run the ANSYS model in a PC with 32 bits and 1.5 GB memory, it is necessary to keep the model within a proper size. For this, fillers and chamfers in the Pro/E geometry were removed. Most of the element sizes are not fine and those parts that have few contributions to the model stiffness were eliminated, such as the PF coil center stack and the vacuum vessel assembly. The complex clamp system for the modular coil was removed, and instead, the modular coils were bonded to the MCWF to assure a stable condition.

The model assumed all contact surfaces were bonded except for the wing interfaces that used frictionless contact elements through the wing bag shims. In the real case, the modular coils, TF coils, and PF coils are not exactly bonded to the structure. Some bolt joints may not be firmly connected on contact surfaces. It is recommended that additional runs by changing contact behavior or by modifying the material properties shall be performed to assess the impact of modeling assumptions.

Stress in the coil is derived from the displacement and the material property. If the accurate stresses of coils are wanted, suitable orthotropic material properties shall be provided and correct contact assumptions shall be presented. To simulate the sliding condition on the MC contact surfaces, an approximate approach may be used by distorting the shear moduli of one of contact part to a very small value without changing the bonded contact behavior. This may be useful for the TF coil shims too.

The currents in the TF and PF coils do not have the highest currents. The stresses in this EM load case do not stand for the critical load case for the TF and PF coils and possibly the TF structure.

Bolt joint contact was assumed to be always bonded. If there was a possibility of partial opening at the joint due to insufficient or unevenly distributed bolts, a standard contact element shall be used.

The stellarator symmetry of the support system makes certain that there are no EM loads transferring to the base support. The analysis did not cover the seismic loads and some interacting forces from the attached components. Therefore, the main load on the support is the dead weight. The support location can be modified to test the best support location.

The selected EM loads from currents at 2T high beta current scenario have the highest currents in the modular coils. Additional load cases may be run to verify the present case is the worst case.

The investigation of the bolt joint was based on the net bolt preload of 45797 lbs. It considered neither the impact of preload variations due to the temperate change, nor the loss of preload due to the creep of insulation materials.

6.0 References

[1] H. Fan, "Nonlinear Analysis of Modular Coil and Shell Structure", NCSX-CALC-14-001-001, February 3, 2006

[2] Engineering Technical Data "C08R00_C8_Ultimate.xls", January 14, 2006, PPPL NCSX web site

[3] B. Nelson, "Requirements for stellarator core support", March 14, 2006

[4] H. Fan, "Descriptions of the NCSX Integrated Model – file6,db", PPPL Email, July 18, 2006

[5] Drawing No. SE132-001 "Centerstack Assembly PF Coils 1, 2, & 3",

[6] F. Dahlgren, Nastran FEA model "model21bbe2a.dat"

[7] T. Kozub, "NCSX Composite Coil Tests", March 15, 2004, PPPL NCSX web site

[8] T. Kozub, "NCSX Composite Coil Tests", April 5, 2004, PPPL NCSX web site

[9] P. Heitzenroeder, "NCSX Product Specification Modular Coil Winding Forms", NCSX-CSPEC-141-03, February, 7, 2006

[10] A. Brooks, "MCWF Toroidal Joint Concerns", PowerPoint presentation attached in the email dated February 28, 2006

[11] A. Brooks, "Analysis of Coil Structure", PowerPoint presentation attached in the email dated July 12, 2006

[12] I. Zatz, Editor, "NCSX Structural Design Criteria, Draft E", May 10, 2004, PPPL web site

[13] NCSX Drawing No. SE132-001 "Centerstack Assembly PF Coils 1, 2, & 3",

[14] F. Dahlgren, Nastran FEA model "model21bbe2a.dat"

[15] P. Heitzenroeder, "FEA Analyses Results of the A1 Casting with Thin Wall Regions", E-Mail attachment, August 8, 2005